UCLA
COMPUTATIONAL AND APPLIED MATHEMATICS

Total Variation Blind Deconvolution

Tony F. Chan
C.K. Wong

November 1996

CAM Report 96-45

Department of Mathematics
University of California, Los Angeles
Los Angeles, CA. 90024-1555

TOTAL VARIATION BLIND DECONVOLUTION

TONY F. CHAN* AND C.K. WONG†

Abstract. In this paper, we present a blind deconvolution algorithm based on the total variational (TV) minimization method proposed in [10]. The motivation for regularizing with the TV norm is that it is extremely effective for recovering edges of images [10] as well as some blurring functions, e.g. motion blur and out-of-focus blur. An alternating minimization (AM) implicit iterative scheme is devised to recover the image and simultaneously identify the point spread function (PSF). Numerical results indicate that the iterative scheme is quite robust, converges very fast (especially for discontinuous blur) and both the image and the PSF can be recovered under the presence of high noise level. Finally, we remark that PSF's without sharp edges, e.g. Gaussian blur, can also be identified through the TV approach.

1. Introduction. It is well-known that recovering the image u (resp. the PSF k) with known PSF (resp. image) is a mathematically ill-posed problem. One of the most successful regularization approaches is the TV regularization method [10] which can effectively recover edges of an image. The mathematical formulations that we used in the image recovery problem is stated as follows [11]:

$$\min_u f(u) \equiv \min_u \frac{1}{2}\|k * u - z\|^2_{L^2(\Omega)} + \alpha \int_\Omega |\nabla u| dx \tag{1}$$

where α is a parameter.

In this paper, we are going to recover u and k without any a *priori* knowledge of the PSF and the image. There are many existing algorithms for simultaneously identify u and k, see for instance, [6, 8, 9, 12, 13]. As this *blind* deconvolution problem is ill-posed with respect to both k and u, You and Kaveh [12] proposed regularizing u and k by considering the joint minimization problem:

$$\min_{u,k} f(u,k) \equiv \min_{u,k} \frac{1}{2}\|k * u - z\|^2_{L^2(\Omega)} + \alpha_1\|u\|^2_{H^1} + \alpha_2\|k\|^2_{H^1}. \tag{2}$$

In our work, we will follow the approach in [12] and combine it with the TV regularization approach (1). More precisely, we regularize both the image and PSF by the TV norm instead of the H^1 norm. The motivation for using TV regularization for the PSF is due to the fact that some PSF's can have edges. Figure 1 shows the four typical PSF's [7] out of which the motion blur and the out-of-focus blur are piecewise constant functions with discontinuities.

* Department of Mathematics, University of California, Los Angeles, 405 Hilgard Avenue, Los Angeles, CA 90095-1555. Email: chan@math.ucla.edu, WWW: http://www.math.ucla.edu/~ chan.

† Department of Mathematics, University of California, Los Angeles, 405 Hilgard Avenue, Los Angeles, CA 90095-1555. Email: ckwong@math.ucla.edu, WWW: http://www.math.ucla.edu/~ ckwong.

The authors are supported by grants ONR-N00017-96-1-0277 and NSF DMS-96-26755.

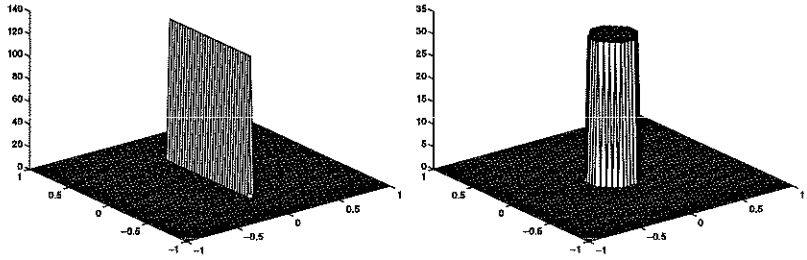

Motion Blur Out of Focus Blur

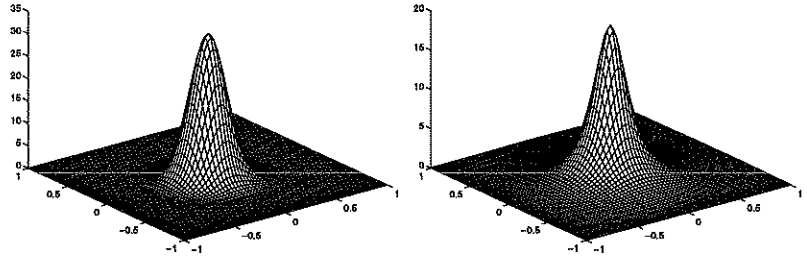

Gaussian Blur Scatter Blur

Figure 1: Some typical PSF

We formulate the blind deconvolution problem as:

$$\min_{u,k} f(u,k) \equiv \min_{u,k} \frac{1}{2}\|k*u-z\|^2_{L^2(\Omega)} + \alpha_1 \int_\Omega |\nabla u| dx + \alpha_2 \int_\Omega |\nabla k| dx. \tag{3}$$

Here α_1 and α_2 are positive parameters which measure the trade off between a good fit and the regularity of the solutions u and k. Such an approach of using TV as a special case of anisotropic diffusion for recovering u and k is also employed independently by You and Kaveh in their more recent work [13]. In our work, we focus on devising fast numerical algorithms for solving the minimization problem (3), which are derived from previous works on numerical methods for solving the image restoration problem (1) when k is known [2, 3, 4, 11]. Moreover, our algorithm can recover both the images and PSF's without any a *priori* information on the PSF (e.g support size). A preliminary version of our work can be found in [5].

In the next section, we will devise an alternating minimization scheme, which is an efficient method for solving (3). §2 will discuss how to choose the regularization parameters α_1 and α_2. Finally, numerical results will be presented in §4.

2. Blind Deconvolution by TV Regularization. To devise numerical schemes for (3), let us write down the first order optimality conditions, namely,

$$\frac{\partial f}{\partial k} = u(-x,-y) * (u*k-z) - \alpha_2 \nabla \cdot \left(\frac{\nabla k}{|\nabla k|}\right) = 0, \qquad x \in \Omega, \tag{4}$$

and

$$\frac{\partial f}{\partial u} = k(-x,-y) * (k*u-z) - \alpha_1 \nabla \cdot \left(\frac{\nabla u}{|\nabla u|}\right) = 0, \qquad x \in \Omega. \tag{5}$$

Here $*$ denotes the convolution operator.

Before we solve for u and k, it is useful to note that for given u (resp. k), $f(u,\cdot)$ (resp. $f(\cdot,k)$) is convex function with respect to k (or u). Therefore, with an initial guess (u^0,k^0) for (u,k), we can minimize (3) by first solving $f(u^0,k^1)\equiv \min_k f(u^0,\cdot)$ using (4) and then $f(u^1,k^1)\equiv \min_u f(\cdot,k^1)$ using (5). Hence, we develop an alternating minimization (AM) algorithm in which the function value $f(u^n,k^n)$ always decreases as n increases. More precisely, the algorithm is stated as follows:

Assume we have u^n and k^n,

- Solve for k^{n+1}

$$u^n(-x,-y)*(u^n*k^{n+1}-z)-\alpha_2\nabla\cdot\left(\frac{\nabla k^{n+1}}{|\nabla k^{n+1}|}\right)=0 \tag{6}$$

- Solve for u^{n+1}

$$k^{n+1}(-x,-y)*(k^{n+1}*u^{n+1}-z)-\alpha_1\nabla\cdot\left(\frac{\nabla u^{n+1}}{|\nabla u^{n+1}|}\right)=0. \tag{7}$$

We remark that a variant of the AM algorithm is to solve (7) first before (6) which corresponds to solve the minimization problem, $f(u^1,k^0)\equiv \min_u f(\cdot,k^0)$ first and then $f(u^1,k^1)\equiv \min_k f(u^1,\cdot)$.

There are some existing numerical methods for solving the above nonlinear type PDEs, for instance, time marching [10], lagged diffusivity fixed point (FP) schemes [11] and primal-dual methods [3]. Due to the robustness and simplicity of implementation of the fixed point algorithm, we apply it to solve (6) and (7) in this paper. The idea of the FP method is to first linearize the nonlinear PDEs (6) and (7) by lagging the diffusive coefficients $\frac{1}{|\nabla k^{n+1}|}$ and $\frac{1}{|\nabla u^{n+1}|}$ by one iteration, and then apply the fixed point method to solve linear problems for k^{n+1} and u^{n+1} respectively. More precisely, the FP iterative method is described as follows:

- solve for k^{n+1} by (iterating on i)

$$u^n(-x,-y)*(u^n*k_{i+1}^{n+1}-z)-\alpha_2\nabla\cdot\left(\frac{\nabla k_{i+1}^{n+1}}{|\nabla k_i^{n+1}|}\right)=0 \tag{8}$$

- solve for u^{n+1} by (iterating on i)

$$k^{n+1}(-x,-y)*(k^{n+1}*u_{i+1}^{n+1}-z)-\alpha_1\nabla\cdot\left(\frac{\nabla u_{i+1}^{n+1}}{|\nabla u_i^{n+1}|}\right)=0. \tag{9}$$

After discretizing (8) and (9), determining k_i^{n+1} and u_i^{n+1} amounts to solving two independent linear systems. It was discussed in [2] how to solve such systems by applying the conjugate gradient (CG) method in which cosine transform preconditioners are used to speed up the convergence rate of the method. The cost per CG iteration will be dominated by two 2D FFT operations.

Unfortunately, numerical experiments indicate that the AM algorithm as stated above in its simplest form, does not always yield physical solutions. It is because the

minimization problem (3) may not have a unique solution. For example, it can be easily observed that if (u, k) is a solution, then so are $(\frac{\alpha_2}{\alpha_1}k, \frac{\alpha_1}{\alpha_2}u)$, $(-u, -k)$, $(u(x \pm c, y \pm d), k(x \mp c, y \mp d))$ for any real constant c and d.

In order to obtain a physical solution, we need to impose conditions on u and k. We have chosen to impose the following conditions:

$$\int_\Omega k(x,y)\, dx\, dy = 1,$$

$$u(x,y), k(x,y) \geq 0, \tag{10}$$

and

$$k \text{ is centrosymmetric}, \qquad \text{i.e. } k(x,y) = k(-x,-y).$$

We remark that besides the above conditions, we don't have any other a *priori* assumptions on the PSF, e.g. the type or the support size of blurring function.

In Figure 2, we try to compare the recovered (1D) images and the identified PSF's before and after imposing the conditions. We observe from Figure 2a that if we don't impose the extra conditions (10), the AM algorithm can converge to the "wrong" solution. Figure 2b shows that the recovered u and k match the original image and PSF after the conditions were imposed. Therefore, it is necessary to add the conditions in order to obtain a reasonable solution. Finally, we remark that we have no proof yet that (10) guarantees uniqueness of (3) but in practice (10) leads to tremendous improvement in performance, robustness and convergence of the algorithm.

In the following, we give the full details of the algorithm:

Alternating Miminization (AM) Algorithm:

• Start with $u^0 = z$ and $k^0 = \delta(x,y)$, the delta function. Assume we have u^n and k^n,

• Solve for k^{n+1} by (iterating on i)

$$u^n(-x,-y) * (u^n * k_{i+1}^{n+1} - z) - \alpha_2 \nabla \cdot \left(\frac{\nabla k_{i+1}^{n+1}}{|\nabla k_i^{n+1}|} \right) = 0$$

Impose

$$k^{n+1}(x,y) = \begin{cases} k^{n+1}(x,y) & \text{if } k^{n+1}(x,y) > 0 \\ 0 & \text{otherwise} \end{cases},$$

$$k(x,y) = (k(x,y) + k(-x,-y))/2$$

$$k^{n+1} = \frac{k^{n+1}}{\int_\Omega k^{n+1}(x,y)\, dx\, dy}.$$

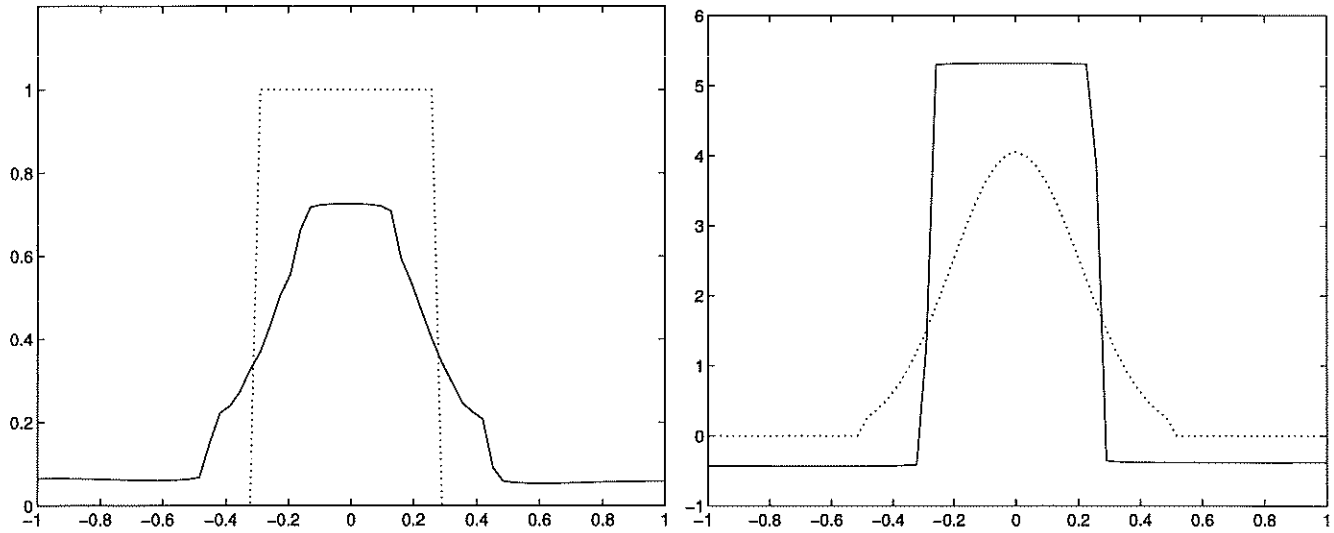

Figure 2a: Recovered image (left) and Identified PSF (right) without constraint
dot: True image/PSF, solid: Recovered image/PSF
$\alpha_1 = 10^{-4}$, $\alpha_2 = 10^{-5}$

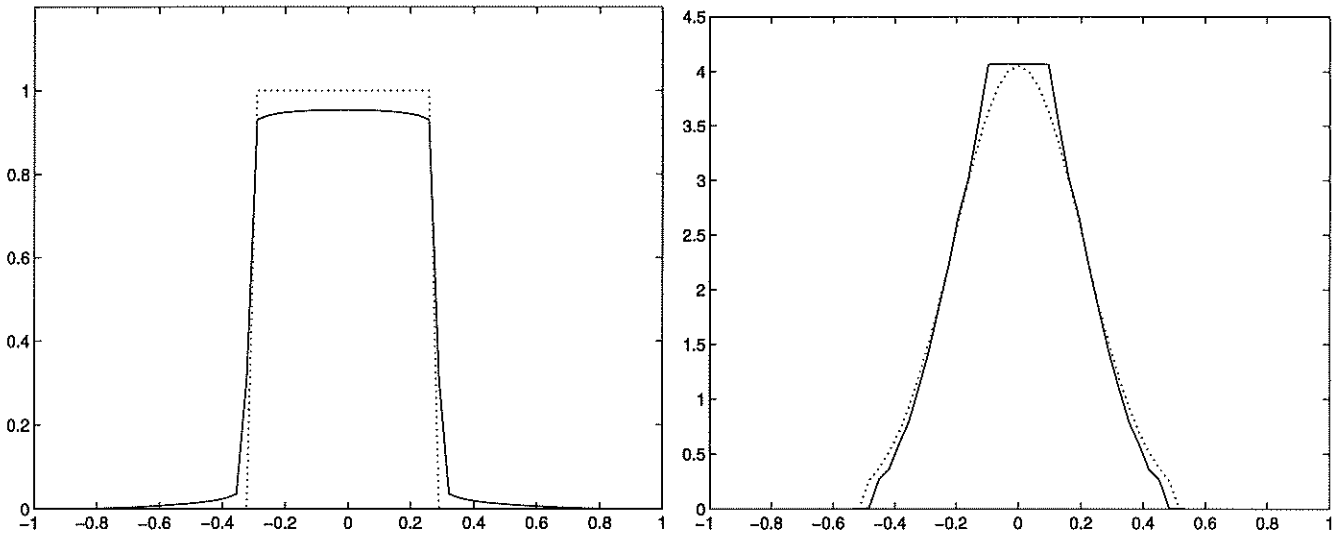

Figure 2b: Recovered image (left) and Identified PSF (right) with constraint
dot: True image/PSF, solid: Recovered image/PSF
$\alpha_1 = 10^{-4}$, $\alpha_2 = 10^{-5}$

Figure 2: Comparison of the recovered images and identified PSF's before and after imposing conditions. Notice that, without constraints, the recovered u and k can be "flipped" versions of the desired solutions.

- Solve for u^{n+1} by (iterating on i)

$$k^{n+1}(-x,-y) * (k^{n+1} * u_{i+1}^{n+1} - z) - \alpha_1 \nabla \cdot \left(\frac{\nabla u_{i+1}^{n+1}}{|\nabla u_i^{n+1}|} \right) = 0.$$

Impose

$$u^{n+1}(x,y) = \begin{cases} u^{n+1}(x,y) & \text{if } u^{n+1}(x,y) > 0 \\ 0 & \text{otherwise.} \end{cases}$$

3. Choice of regularization parameters. In this section, we are going to point out that the regularization parameters α_1 and α_2 respectively depends directly on the noise level and the severity of the blur in the observed image. To understand this, let us first consider the following noise-constrained minimization problem:

$$\min_{u,k} \int (|\nabla u| + \alpha |\nabla k|) \, dx \tag{11}$$

subject to

$$\|k * u - z\|^2 = \sigma^2$$

where σ is the noise level. The Lagrangian for (11) is

$$f(u,k) = \int |\nabla u| \; + \; \alpha \, |\nabla k| \, dx \; + \; \frac{\lambda}{2} (\|k * u - z\|^2 - \sigma^2)$$

where λ is the Lagrange multiplier. It follows that the minimization problems (3) and (11) are identical if $\alpha_1 = 2/\lambda$ and $\alpha_2 = 2\alpha/\lambda$. By making use of the noise-constrained formulation (11), we are going to describe some guidelines for selecting the parameters, α_1 and α_2.

Clearly, if the SNR is small (or σ is large), then λ should be small so that $\int |\nabla u|$ is sufficiently large to regularize the image. Therefore, a good heuristic is to assume that λ is proportional to the SNR. Hence, we expect $\alpha_1 = 2/\lambda$ to be directly proportional to the noise level σ and the numerics we have so far also support this argument, see [11]. The parameter α_2, on the other hand, controls the support or the spread of the PSF. When α_2 gets bigger, the TV regularization for k, $\int |\nabla k|$, is required to be small in order to minimize (11). Therefore, the peak of k will be lower when α_2 gets bigger. Since we impose the constraint, $\int k = 1$, the PSF must spread out. Hence, α_2 can be chosen proportionately according to the amount of desired deblurring.

In our numerical experiments, the initial guess for u is chosen (unless stated otherwise) to be the observed image z as it is the only available approximation of u. The initial guess for k is chosen to be the delta function $\delta(x,y)$ because in the case of no blurring, $\delta(x,y)$ would be the expected PSF (which can be achieved by setting $\alpha_2 = 0$). If the recovered image isn't deblurred enough, we restart the AM algorithm with a larger value of α_2, which increases the support of the identified PSF, until a reasonable recovered image appears. We will illustrate the above ideas experimentally in the next section.

Finally, we can combine this idea with the method of continuation on α_2. More precisely, we start the algorithm with a small α_2 and $u^0 = z$ and $k^0 = \delta$. When we restart the AM algorithm with a larger α_2, we can make use of the solution (u, k) from the smaller α_2 as an initial guess, which should be a better approximation to the true solution than (u^0, k^0). We have not explored this idea fully in this paper.

4. Numerical results. In this section, numerical results are presented to illustrate the efficiency and the effectiveness of the AM algorithm. The results show that the image and PSF can be recovered even under the presence of high noise level with just a several number of AM iterations. We will also compare images that are recovered by using the TV norm with those obtained by the H^1 norm. Moreover, we will perform a experiment to support the continuation idea proposed in §3 on how to choose the regularization parameter α_2.

The test image is the satellite image shown in Figure 3 from Phillips Laboratory at Kirkland Air Force Base, New Mexico and was provided to us by Professor Robert Plemmons of Wake Forest University. The image originally consists of 256-by-256 pixels. To simplify the computational work, we down sample it to become a 127-by-127 pixels image. Currently, our codes are written in MATLAB with machine precision roughly equal to 10^{-16}. At each step of the AM algorithm, we iterate the FP iteration 10 times. Within each FP iteration, we are required to solve a linear system and we do it by applying the CG method. In order to speed up the convergence rate of the CG iteration, we preconditioned the linear system by a cosine transform preconditioner that we developed earlier [2]. The CG iteration is stopped when the relative residual is less than 0.1. We have find that such a low tolerance for the inner iteration is good enough and is most effective for the FP method.

Figure 4 illustrates the ideas on choosing the regularization parameters proposed in §3. Figure 4a shows the PSF, which is a out-of-focus blur, and the blurred image (without noise). Figure 4b shows the recovered images and the identified PSF's for varies α_2. The parameter α_1 is fixed at 2×10^{-6} as it produces the best recovered image in case the PSF is known. We see that the recovered PSF has increasing support as α_2 increases. When $\alpha_2 = 10^{-6}$ or 10^{-7}, the support of the identified PSF's are smaller than the true PSF (c.f. Figure 4a), and the recovered images are only slightly deblurred. When $\alpha_2 = 10^{-5}$, the recovered image is in sharp focus. If we further increase the value of α_2, says to 10^{-4}, the spread of the PSF becomes too large and the recovered image becomes irregular. Therefore, by varying α_2, we can easily pick up the appropriate recovered image.

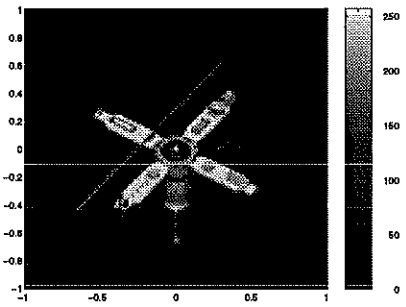

Figure 3: Satellite image

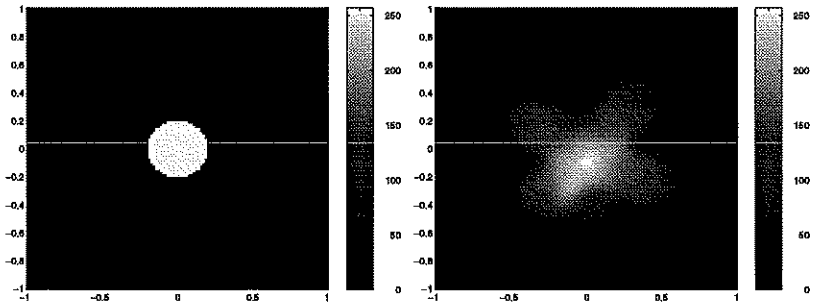

Figure 4a: PSF: out of focus blur (left) and blurred image (right)

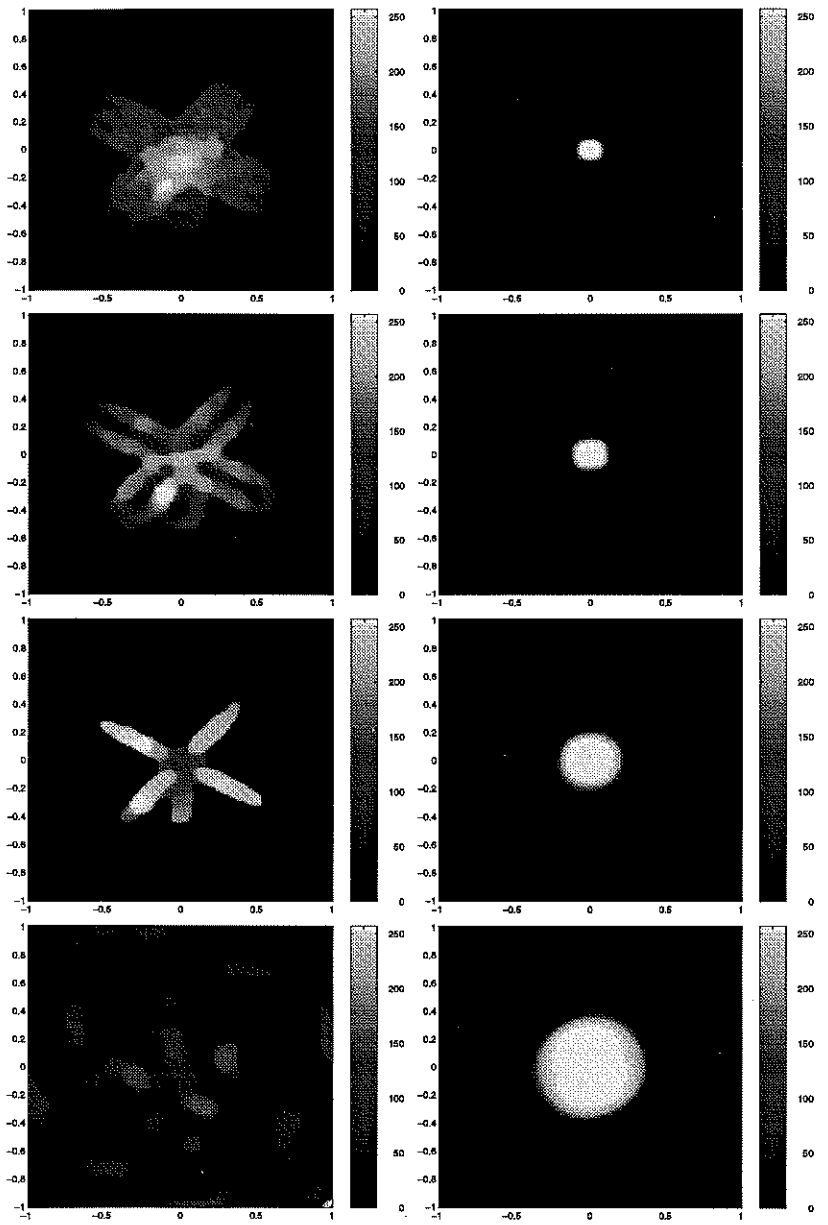

Figure 4b: Recovered images (left) and PSF's (right) with $\alpha_2 = 10^{-7}$, 10^{-6}, 10^{-5}, 10^{-4}, (from top to bottom) and $\alpha_1 = 2 \times 10^{-6}$. Observe that as α_2 increases, the spread of the identified PSF also increases. When α_2 is too small (e.g. $\alpha_2 = 10^{-6}$ or 10^{-7}), the images are not sufficiently deblurred. When $\alpha = 10^{-5}$, the image is in sharp focus. When we further increase α_2, the image becomes irregular.

In Figure 5, we show that the AM algorithm can effectively recover images and identifying PSF's even in the presence of high noise level. Figures 5a shows the observed image which is blurred by the out-of-focus blur shown in Figure 4a. The observed image in Figure 5b is in addition polluted by Gaussian noise with SNR = 5. After performing 3 AM iterations on both the observed images, we obtain very good recovered images. In particular, we can see in Figure 5a that an antenna appears in the recovered image (c.f. Figure 4a). Moreover, even with a high noise level (Figure 5b), the AM algorithm can still recover a very sharp image. In Figure 5c, we display the images that are recovered from the TV regularization scheme (1) assuming the exact PSF is known. Comparing the recovered images in Figure 5a,b,c, we find that even if we don't know the exact PSF, the AM algorithm can still recover images that are almost as good as that recovered with the exact PSF. This experiment demonstrates the robustness of the AM algorithm.

In Figure 6, we display the recovered images after 0, 1, 2, 3 AM iterations. We see that after the first AM iteration, we already have a very good recovered image. Hence, the AM algorithm is a efficient method for minimizing (3).

Figure 7 tries to justify our use of the TV instead of the H^1 regularization for u in (1). In this experiment, we assume the PSF is known and we compare the images recovered by the TV and the H^1 regularization. The observed image in Figure 7a is obtained by blurring the satellite image by the PSF shown in Figure 4a and then polluted with noise (SNR = 10). Figure 7b,c show the recovered images obtained by using the TV and the H^1 norm for various regularization parameters α. The H^1 regularization produces its best image when α is 10^{-2} while for the TV regularization it is when α is 10^{-5}. We see that the best recovered image for the TV regularization is better than that of the H^1, as the former can effectively reproduce edges and give sharp contrast.

Figure 8 shows the recovered u and k by minimizing (3) *except* we replaced the TV norm in k by the H^1 norm. In the experiment, α_1 is fixed at the value 2×10^{-6} and we vary α_2. We can observe that the recovered images are not as good as using the TV norm for k. This justifies why we use the TV norm when recovering k instead of the H^1 norm.

Finally we show in Figure 9 that the TV regularization approach is also good for identifying PSF's without edges (e.g. the Gaussian blur, $g_\gamma(x,y) = \exp(-\gamma(x^2+y^2))$). Figure 9a shows the observed image which is blurred by Gaussian blur (with $\gamma = 200$) without noise. Unfortunately, we observe that the convergence rate of the AM algorithm is slower than in the case of out-of-focus blur. For example, Figure 9b shows that there is still a lot of improvement in the recovered image from 3 to 35 AM iterations. This is almost surely due to the ill-conditioning of the Gaussian blur operator. Although the PSF k is not perfectly identified, we can still recover an image u which is even better than the image obtained by solving (3) with H^1 regularization in k (c.f. Figure 9c). However, we should note, however, that the AM algorithm converges much faster when we use H^1 regularizatin on k. One way to speed up the convergence rate of the AM algorithm is by using a good initial guess for k (e.g. a guide star). In this case, we perform a variant of the AM algorithm, in which at each AM step, we recover u before

k. Figure 10a shows that if we make use as initial guess for k a blurring operator of the correct type (Gaussian in this case) but with a slightly wrong parameter γ ($\gamma = 300$ instead of $\gamma = 200$), then we can obtain a better solution than starting with the generic delta function (c.f. Figure 9b). In fact, if our initial guess for k happens to be the exact solution g_{200} (see Figure 10b), the algorithm will leave this alone and produce almost an exact solution in 3 iterations.

We conclude that the AM/FP algorithm is a robust and efficient method for solving the minimization problem (3) and we have justified the choice of using the TV norm for regularizating u and k instead of the H^1 norm. The case of highly ill-conditioned blurring operators such as Gaussian blur still requires more investigation to improve its rate of convergence.

Acknowledgment: The authors wish to thank Dr. Guillermo Sapiro for helpful discussions and bringing the paper [13] to our attention.

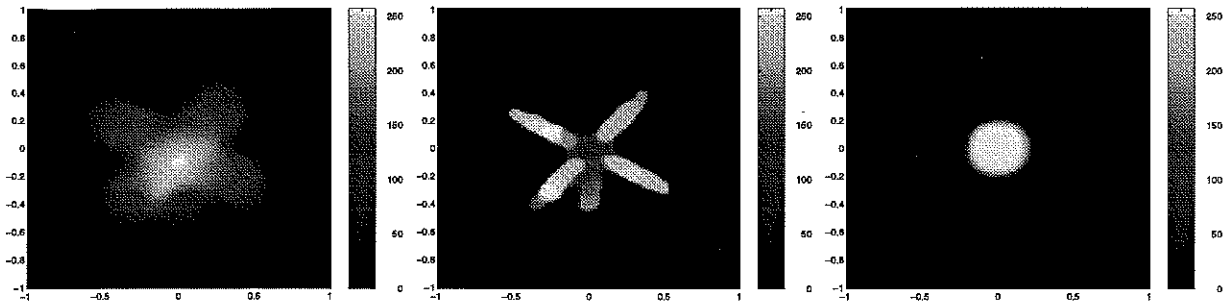

Figure 5a: Observed (left) and recovered (middle) images and identified PSF (right) after 3 AM iterations
$\alpha_1 = 2 \times 10^{-6}$, $\alpha_2 = 1.5 \times 10^{-5}$, SNR=$\infty$

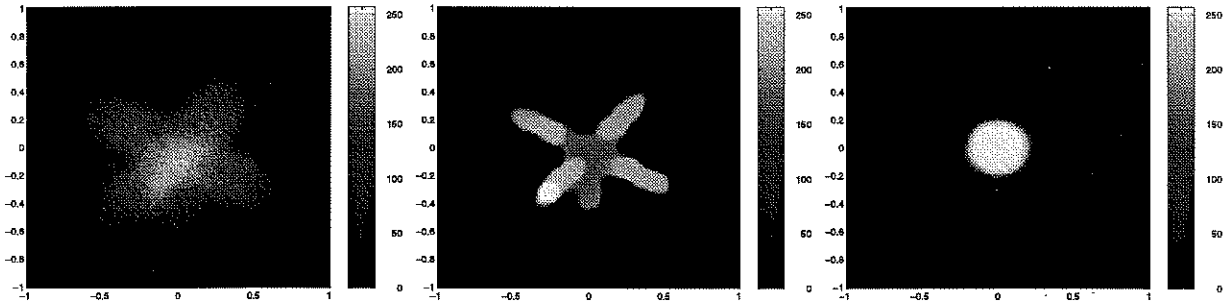

Figure 5b: Observed (left) and recovered (middle) images and identified PSF (right) after 3 AM iterations
$\alpha_1 = 2 \times 10^{-5}$, $\alpha_2 = 1.5 \times 10^{-5}$, SNR=5

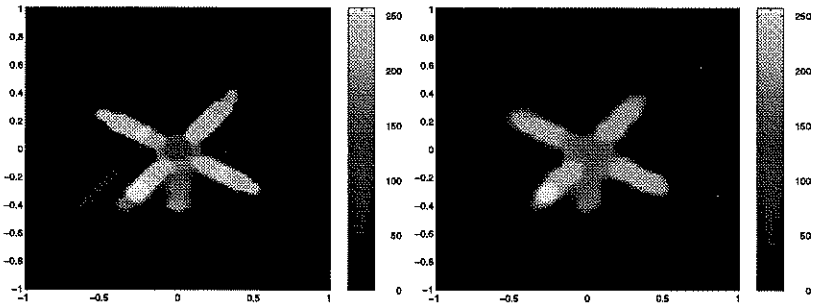

Figure 5c: Recovered image by (1) with known PSF
Left: SNR $= \infty$, $\alpha = 2 \times 10^{-6}$, Right: SNR $= 5$, $\alpha = 2 \times 10^{-5}$

Figure 5: These figures shows that the AM algorithm can recover images with high noise level and that the recovered images are almost as good as that recovered with the exact PSF.

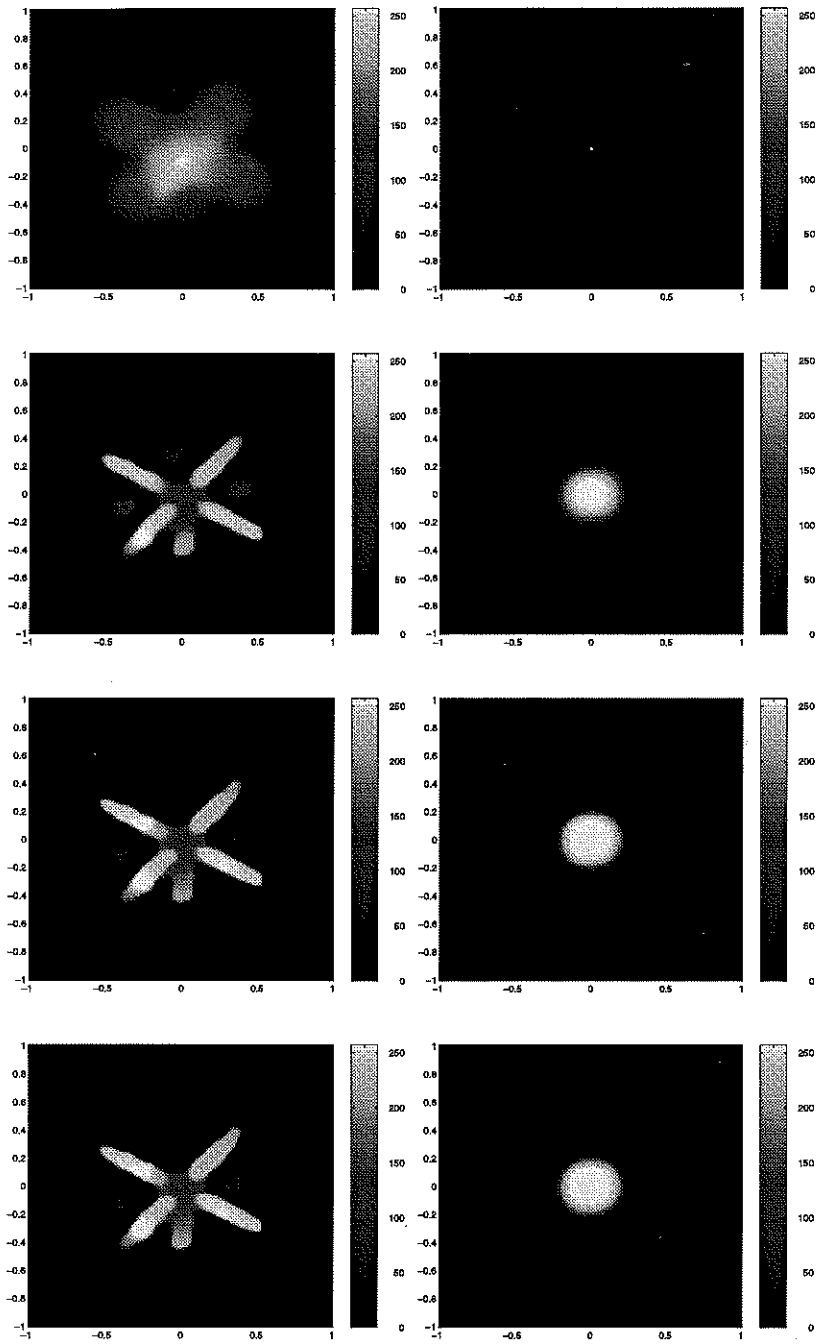

Figure 6: Recovered images and PSFs after 0, 1, 2, 3 AM iterations (from top to bottom). These figures show that the AM algorithm can recover very good images after only a few iterations.

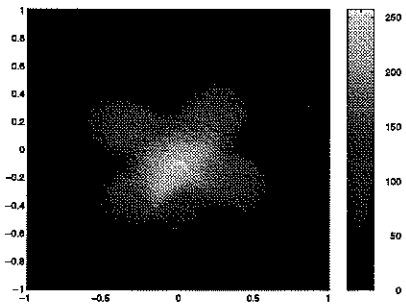

Figure 7a: Observed image

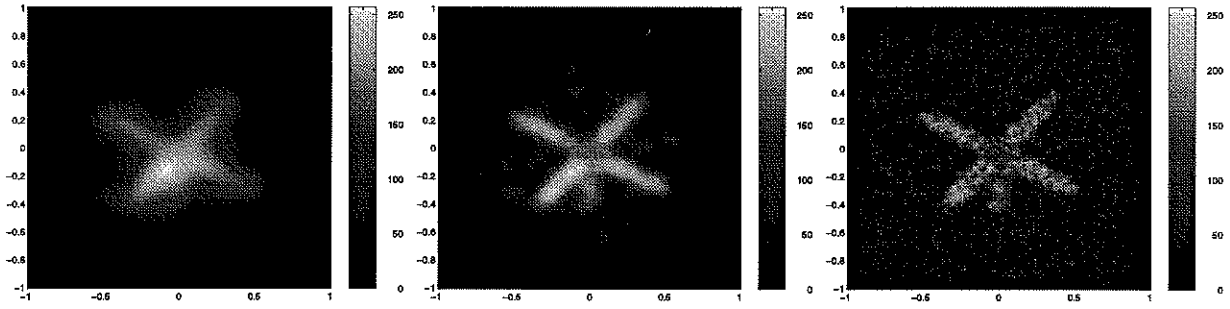

Figure 7b: Image recovered by H^1 norm with given PSF
$\alpha = 10^{-1},\ 10^{-2},\ 10^{-3}$, (from left to right)

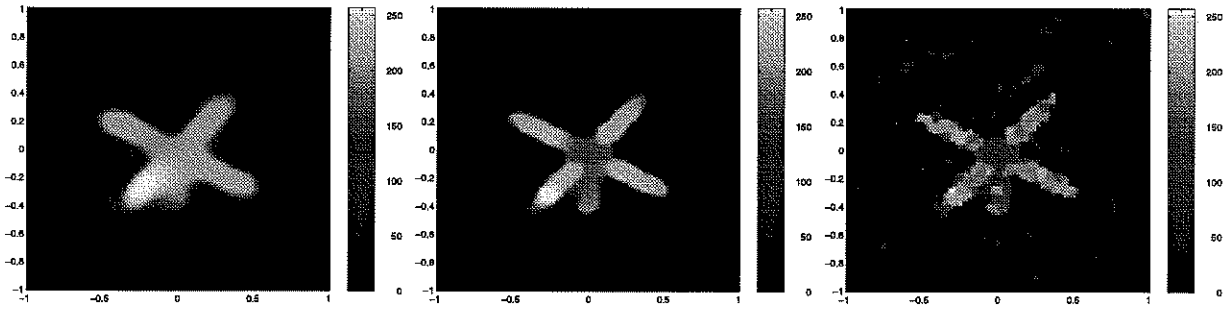

Figure 7c: Image recovered by TV norm with given PSF
regular. paramter, $\alpha = 10^{-4},\ 10^{-5},\ 10^{-6}$, (from left to right)

Figure 7: Comparison of using TV norm and H^1 norm in image recovery problem. Notice that TV is better than H^1 as it can effectively reproduce edges and give sharper contrast.

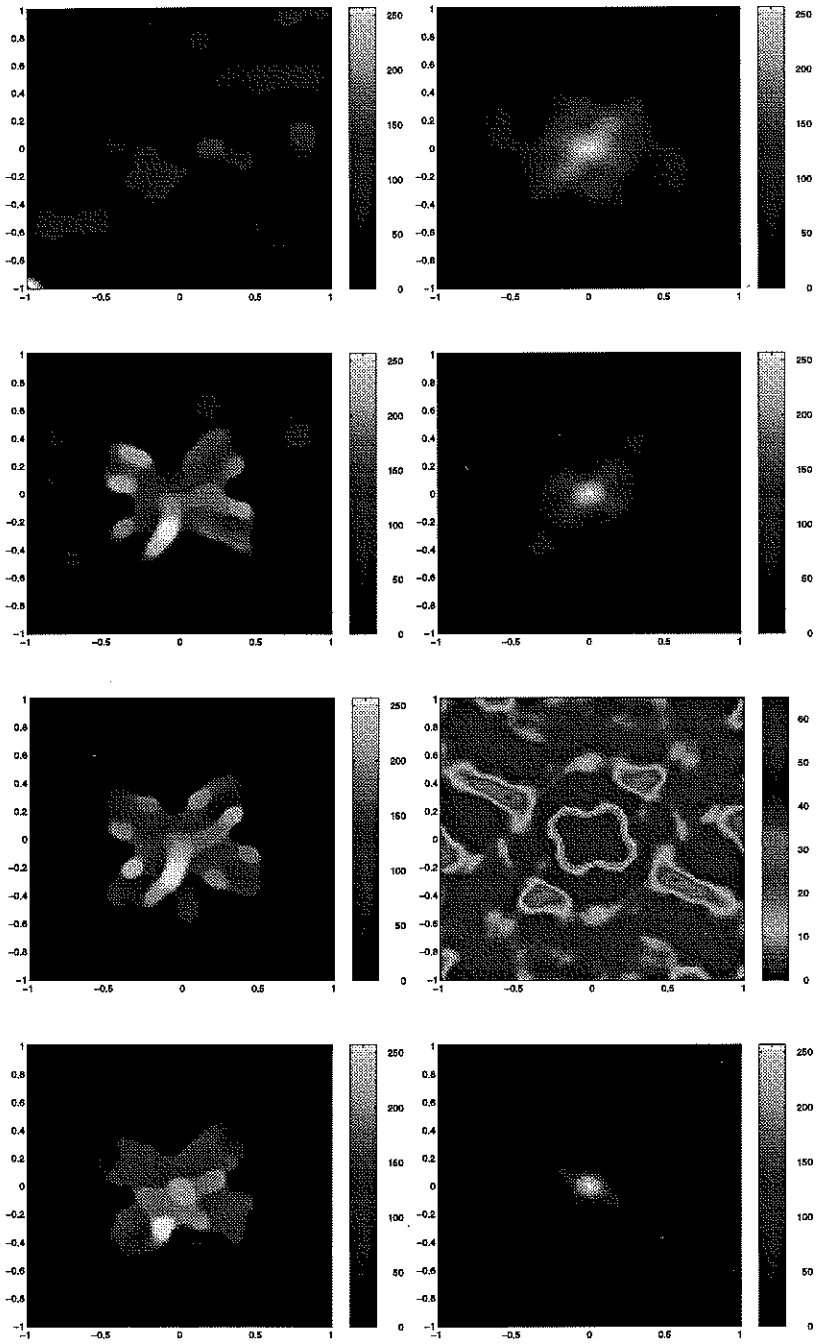

Figure 8: Recovered image (left) and PSF (right) using TV norm in u and H^1 norm in k, with $\alpha_2 = 10^{-6},\ 10^{-5},\ 10^{-4},\ 10^{-3}$ (from top to bottom). Observe that H^1 in k is not as good as TV in k.

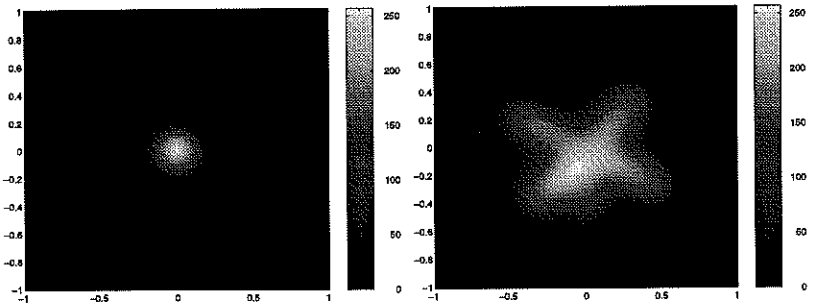

Figure 9a: PSF: Gaussian blur (left), Observed image (right)

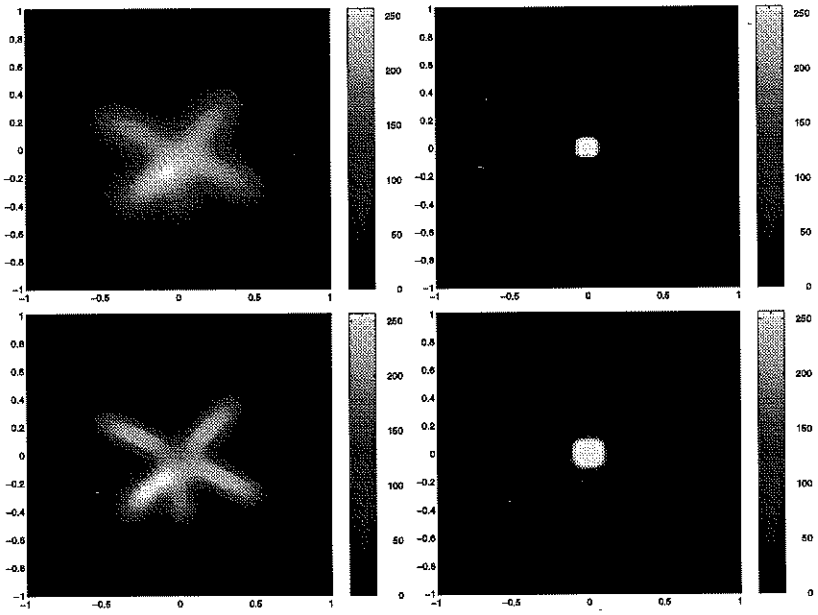

Figure 9b: Recovered image (left) and PSF (right) after 3 (top) and 35 (bottom) AM iterations. TV norm in u and k. $\alpha_1 = 10^{-7}$, $\alpha_2 = 10^{-8}$.

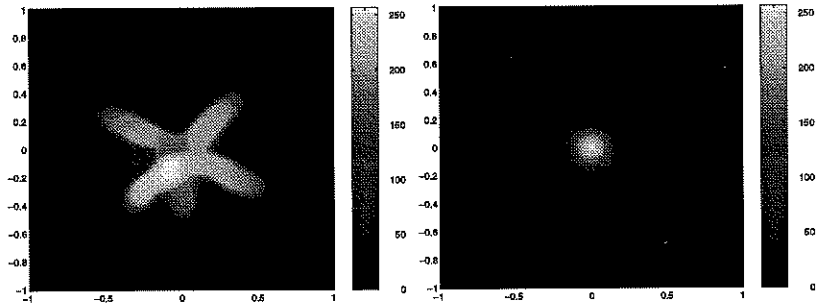

Figure 9c: Recovered image (left) and PSF (right) after 3 AM steps TV norm in u and H^1 norm in k. $\alpha_1 = 10^{-6}$, $\alpha_2 = 10^{-6}$

Figure 9: Comparison of using TV norm and H^1 norm for k. Although the convergence in this case is not fast, TV is still good for recovering PSF without edges. The H^1 norm on k solution u is not as good as the "converged" TV solution but it converges much faster.

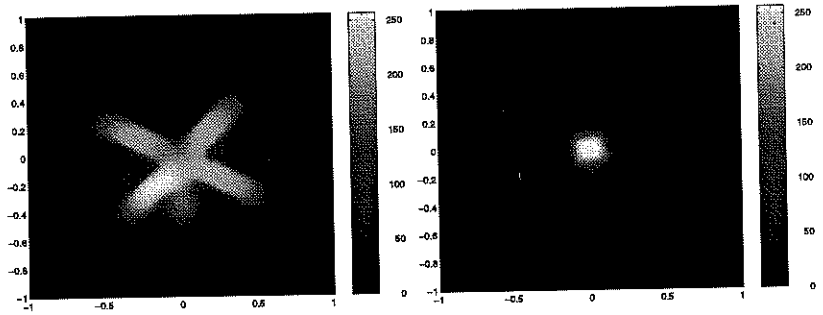

Figure 10a: Recovered images and PSF's after 5 AM iterations with $k^0 = g_{300}$. $\alpha_1 = 10^{-7}$, $\alpha_2 = 10^{-8}$

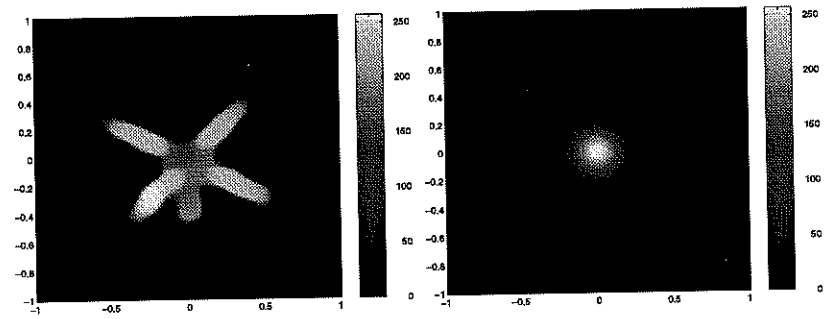

Figure 10b: Recovered images and PSF's after 5 AM iterations with initial guess $k^0 = g_{200}$. $\alpha_1 = 10^{-7}$, $\alpha_2 = 10^{-8}$

Figure 10: Recovered u and k when AM starts with good initial guess. Observe that the convergence of the AM algorithm improves a lot if we have a good approximation to k^0.

REFERENCES

[1] R. Acar and C. Vogel, *Analysis of Bounded Variation Penalty Methods*, Inverse Problems, Vol. 10 (1994), pp. 1217–1229.

[2] R. Chan, T. Chan and C. Wong. *Cosine Transform Based Preconditioners for Total Variation Minimization Problems in Image Processing.* In S. Margenov and P. Vassilevski, editors. *Iterative Methods in Linear Algebra,* II, pp. 311–329, IMACS Series in Computational and Applied Math., V3, IMACS, NJ, 1996.

[3] T. Chan, G. Golub and P. Mulet, *A nonlinear primal-dual method for TV-based image restoration,*, in ICAOS'96, 12th Int'l Conf. on Analysis and Optimization of systems: Images, wavelets and PDE's, Paris, June 26– 28, 1996, M. Berger, R. Deriche, I. Herlin, J. Jaffre, and J. Morel, eds., no. 219 in Lecture Notes in Control and Information Sciences, 1996, pp. 241 – 252.

[4] T. Chan and P. Mulet, *Iterative Methods for Total Variation Image Restoration*, Proceedings of Winter School on Iterative Methods, the Chinese University of Hong Kong, Dec 1995, Spring Verlag, Singapore.

[5] T. Chan and C. Wong, *Total Variation Blind Deconvolution*, Virtual Proc. of ONR workshop, Sep. 4–6 1996. WWW: http://www.math.ucla.edu/ ~ blomgren/Workshop96/

[6] D. Fish, A. Brinicombe and E. Pike, *Blind deconvolution by means of the Richardson-Lucy algorithm*, J. Opt. Soc. Am. A Vol. 12, No.1 January 1996.

[7] R. L. Lagendijk and J. Biemond, Iterative Identification and Restoration of Images, *Kluwer Academic Publishers*, 1991

[8] R.L. Lagendijk, A. M. Tekalp and J. Biemond, *Maximum likelihood image and blur identification: a unifying approach,* Opt. Eng. 29(4), 1990.

[9] R.L. Lagendijk, J. Biemond and D. E. Boekee, *Identification and restoration of noisy blurred images using the expectation-maximization algorithm*, IEEE Trans. Acoust. Speech Sig. Proc. 1990.

[10] L. Rudin, S. Osher and E. Fatemi, *Nonlinear Total Variation Based Noise Removal Algorithms*, Physica D., 60 (1992), pp. 259–268.

[11] C. Vogel and M. Oman, *Iterative Methods for Total Variation Denoising*, SIAM J. Sci. Statist. Comput., to appear.

[12] Y. You and M. Kaveh, *A regularization approach to joint blur identification and image restoration*, IEEE Transactions on Image Processing, Vol 5 pp. 416–428, March 1996.

[13] Y. You and M. Kaveh, *Anisotropic Blind Image Restoration* IEEE International Conference Image Proc. Lausanne '96.